This is a repository copy of *The evolution of cutting forces during slot milling of unidirectional carbon fiber reinforced polymer (UD-CFRP) composites*.

White Rose Research Online URL for this paper:
http://eprints.whiterose.ac.uk/155018/

Version: Published Version

Proceedings Paper:

Sheikh-Ahmad, J., El-Hofy, M., Almaskari, F. et al. (2 more authors) (2019) The evolution of cutting forces during slot milling of unidirectional carbon fiber reinforced polymer (UD-CFRP) composites. In: Kerrigan, K., Mativenga, P. and El-Dessouky, H., (eds.) Procedia CIRP. 2nd CIRP Conference on Composite Material Parts Manufacturing, 10-11 Oct 2019, Sheffield, UK. Elsevier , pp. 127-132.

https://doi.org/10.1016/j.procir.2019.09.043

Reuse
This article is distributed under the terms of the Creative Commons Attribution-NonCommercial-NoDerivs (CC BY-NC-ND) licence. This licence only allows you to download this work and share it with others as long as you credit the authors, but you can’t change the article in any way or use it commercially. More information and the full terms of the licence here: https://creativecommons.org/licenses/

Takedown
If you consider content in White Rose Research Online to be in breach of UK law, please notify us by emailing eprints@whiterose.ac.uk including the URL of the record and the reason for the withdrawal request.

eprints@whiterose.ac.uk
https://eprints.whiterose.ac.uk/

Available online at www.sciencedirect.com

ScienceDirect

Procedia CIRP 85 (2019) 124–129

www.elsevier.com/locate/procedia

2nd CIRP Conference on Composite Material Parts Manufacturing (CIRP-CCMPM 2019)

The evolution of cutting forces during slot milling of unidirectional carbon fiber reinforced polymer (UD-CFRP) composites

Jamal Sheikh-Ahmad[a,*], Mohamed El-Hofy[b], Fahad Almaskari[c], Kevin Kerrigan[b], Yoshihiro Takikawa[d]

[a]*Department of Mechanical Engineering, Khalifa University of Science and Technology, SAN Campus, Abu Dhabi, United Arab Emirates*
[b]*AMRC with Boeing, The Universality of Sheffield, Advanced Manufacturing Park, Wallis way, Catcliffe, Rotherham, S60 5TZ, UK*
[c]*Department of Aerospace Engineering, Khalifa University of Science and Technology, Main Campus, Abu Dhabi, United Arab Emirates*
[d]*OSG Corporation, 3-22 Honnogahara, Toyokawa, Aichi 442-8543, Japan*

* Corresponding author. Tel.: 971-2-607-5338. *E-mail address:* jamal.ahmad@ku.ac.ae

Abstract

Cutting forces generated during traditional machining of fiber reinforced polymer composites play an important role in determining machined surface quality. The cutting force signals also provide a live indicator of the dynamic behavior of the chip formation process. Cutting forces in machining FRPs are dependent primarily on the instantaneous fiber cutting angle, chip thickness, cutting edge geometry and the current state of cutting edge wear. In this study, effects of the cutting edge rake angle and tool wear on cutting force evolution during slot milling of unidirectional carbon fiber reinforced polymer (UD-CFRP) composite was investigated. The cutting forces were measured in the feed and normal directions and then transformed to the tangential and radial directions of the tool path. A simplified cutting force model consisting of a shearing region and a pressing was used to determine the shearing and friction force components. This allowed determination of the friction coefficient on the clearance face of the tool. It was found that the friction coefficient varied significantly with rake angle and fiber cutting angle. The effect of rake angle on cutting forces is more discernable in the shearing region with positive rake angle tool providing the most efficient cutting. Furthermore, correlations were found between machining damage and the magnitude and orientation of the resultant shearing force.

© 2020 The Authors. Published by Elsevier B.V.
This is an open access article under the CC BY-NC-ND license (http://creativecommons.org/licenses/by-nc-nd/4.0/)
Peer-review under responsibility of the scientific committee of the 2nd CIRP Conference on Composite Material Parts Manufacturing.

Keywords: Slot milling; CFRP; cutting forces; fiber cutting angle; rake angle; friction coefficient; machining damage.

1. Introduction

The cutting forces generated during the machining of fiber reinforced composites are of major concern because of their direct prelateship to delamination damage. Excessive forces normal to the stacking plane promote delamination by separation of the unsupported top and/or bottom plies of the laminate. Generally, the cutting forces in machining are dependent on the cutting tool geometry as well as process parameters such as spindle speed and feed rate with the later defining the uncut chip thickness. Of particular interest when using a defined geometry tool, is the effect of rake angle on cutting forces owing to its effect on the mode of fiber cutting.

Several studies have previously addressed the cutting force behavior and its relationship to chip formation and machining damage in orthogonal cutting of fiber reinforced composites. Kaneeda [1], Wang et al. [2] and Wang ad Zhang [3] delineating the important roles of the cutting tool geometry and the fiber cutting angle in determining the chip formation mechanism. Hintze et al. [4] studied the occurrence of fiber overhang when slot milling unidirectional CFRP and showed that machining damage is promoted by tool wear and that it occurs in a critical fiber cutting angle range ($90^\circ \leq \theta \leq 180^\circ$). Damage might also propagate outside this critical range under certain conditions. The works of Wang et al. [5] and Voss et al. [6] also showed that machining damage might occur outside this critical range. In the latter study, it was shown that the

2212-8271 © 2020 The Authors. Published by Elsevier B.V.
This is an open access article under the CC BY-NC-ND license (http://creativecommons.org/licenses/by-nc-nd/4.0/)
Peer-review under responsibility of the scientific committee of the 2nd CIRP Conference on Composite Material Parts Manufacturing.
10.1016/j.procir.2019.09.043

formation of fiber overhang is promoted by high resultant cutting forces. Furthermore, an increase in the cutting edge rake angle was shown to increase machining quality due to a decrease in the resultant cutting forces and the more favorable mode of chip formation. It is imperative to note here that the resultant cutting force considered in [6] is the apparent total force. However, the total cutting force is composed of an active force component, which is responsible for fiber cutting and a passive component representing the friction on the clearance face. Zhang et al. [7] proposed a mechanics force prediction model in which the cutting zone ahead of the cutting tool was divided into three regions, namely, chipping, pressing and bouncing. The resultant cutting force in machining is therefore composed of contributions from these three regions. This model was further simplified by Maegawa et al. [8] by combining the pressing and bouncing regions into one region where friction is dominant. Nonetheless, it is not clear from these previous studies as of which of the force components actually promotes the occurrence of delamination.

The friction behavior in machining CFRPs is an important phenomenon because of its effect on the cutting forces, tool wear progression and cutting temperatures. Therefore, an accurate estimation of the friction coefficient is a requirement for both analytical and numerical modeling of the machining process. Tribometers can measure the friction coefficient at different loads, temperatures or sliding velocities which help identify the optimum cutting parameters. However, calculating friction coefficient from cutting force measurement is an alternative. Up to date, there are only a few attempts to quantify the friction behavior of FRPs under realistic machining conditions. Nayak et al. [9] studied the friction behavior of UD-GFRP blanks of different fiber orientations on a rotating HSS disk and reported that the friction coefficient increased with increasing inclination angle of the fibers. Klinkova et al. [10] studied the influence of sliding velocity on the friction coefficient between TiN coated carbide and randomly structured CFRP. Voss et al. [11] utilized a cutting tribometer and showed that the coefficient of friction varied only slightly with fiber orientation in the sliding of diamond coated carbide pin against UD-CFRP. Xu et al. [12] investigated the contribution of elastic springback to the apparent friction coefficient between tungsten carbide tool and multidirectional CFRP. It was determined that the elastic friction coefficient is very small when compared to the apparent coefficient.

The present work utilizes a slot milling experiment to study the cutting force evolution and friction behavior during machining UD-CFRP using tools with –ve, 0 and +ve rake angles. The simplified cutting model in [8] was used to evaluate the cutting forces in the two regions of the model. This allowed a more realistic estimation of the friction coefficient. The relationship between the cutting forces, tool geometry and machining damage is also delineated.

2. Materials and Methods

Slot milling experiments were conducted on unidirectional CFRP laminates in dry cutting environment. The cutting tool was a single straight flute uncoated tungsten carbide cutter with a diameter of 10 mm. Three rake angles were used in the slot milling operation, namely α = -15, 0 and 15°. All tools had a clearance angle of 15° and a nose radius of less than 4.0 μm. The cutting edge was perpendicular to the cutting velocity vector, thus ensuring orthogonal cutting. Slot milling was performed on 3.0 mm thick unidirectional CFRP laminates and the length of cut was approximately 20 mm. A new cutting edge was used for each experiment and the cutting edge was examined before and after cutting. The CFRP blank dimensions were 80 mm in length and 60 mm in width. The workpiece material was an intermediate modulus unidirectional continuous carbon fiber reinforced epoxy composite (IM6/3501-6) with 62% fiber volume fraction. The cutting forces in the feed and normal directions were measured using a Kistler (Type 9257B) piezoelectric dynamometer at a sampling frequency of 24kHz. The cutting force signals were conditioned and filtered by a 1kHz low pass filter using Kistler (Type 5070) charge amplifier. Images for quality assessment were captured using Zeiss Smartzoom 5 microscope.

Figure 1 shows the different angle definitions used in this study. The cutter rotation (immersion) angle, φ, is measured in a clockwise direction from entry. The laminate orientation angle, ψ, is measured clockwise from the feed direction to the fiber. Four different laminate orientations ψ = 0°, 45°, 90° and 135° were used. The fiber cutting angle, θ, is measured in a clockwise direction from the cutting velocity vector to the fiber. In milling, the uncut chip thickness, a_c, fiber cutting angle, θ, and cutting configuration (up-milling vs. down-milling) change continuously with increasing the rotation angle. The mode of chip formation and the cutting forces depend greatly on the fiber cutting angle [1, 2]. The uncut chip thickness is related to the feed speed, F, and rotation speed, N, by the relationship,

$$a_c = f_z \sin(\varphi) = \frac{F}{N} \sin(\varphi) \qquad (1)$$

where f_z is the feed per tooth. The spindle speed and feed speed were held constant at 4000 rpm and 100 mm/min for all milling experiments.

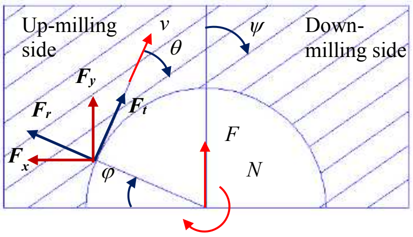

Figure 1. Slot milling geometry and the different angle conventions.

Table 1 shows typical fiber cutting angles for the different laminate orientations and different cutter rotation angles. It can be seen that for any given laminate orientation, the fiber cutting angle spans the whole spectrum from 0 to 180°, and thus, different chip formation modes occur as the tool rotates from entry to exit. The cutting configuration also changes with rotation angle. For rotation angles less than 90°, the cutting velocity vector and the tool feed vector are both in the same direction and the cutter is engaged in up-milling. For rotation angles greater than 90°, the cutting velocity vector and the tool feed vector are in opposite directions and the cutter is engaged in down-milling.

Table 1. Variation of fiber cutting angle with rotation angle and laminate orientation.

	θ (Deg)			
***φ* (Deg)**	**ψ = 0˚**	**ψ = 45˚**	**ψ = 90˚**	**ψ = 135˚**
0	0, 180	45	90	135
45	135	0, 180	45	90
90	90	135	0, 180	45
135	45	90	135	0, 180
180	0, 180	45	90	135

3. Results and Discussion

3.1. The cutting force cycle

The cutting forces in the feed and normal direction for one tool rotation were obtained by averaging 10 cutting cycles after the full engagement of the cutter diameter in the workpiece. These forces were then transformed to the tangential and radial directions using the transformation equation (3).

$$\begin{pmatrix}F_t\\ F_r\end{pmatrix} = \begin{bmatrix}-sin(\varphi) & cos(\varphi)\\ cos(\varphi) & sin(\varphi)\end{bmatrix}\begin{pmatrix}F_x\\ F_y\end{pmatrix} \qquad (3)$$

Figure 2 shows the transformed cutting force cycles for the four laminates and three rake angles used in this study. Generally, the cutting forces increased with rotation angle to a maximum and then decreased to almost zero level at cutting edge exit. This is somewhat in accordance with the variation in the uncut chip thickness, which follows a sine wave as indicated by eq.(1). However, the force signals deviate greatly from the perfect sine wave due to the effects of a continuously changing fiber cutting angle and the noise caused by low frequency dynamic response of the tool/fixture system. FFT analysis of the force signals revealed that low frequency oscillations of the cutting forces occurred mainly at the low order harmonics of the tool passing frequency (nω, where n = 1,…4). Therefore, the exact form of the cutting force cycle cannot be obtained from the collected force signals as is. Nevertheless, the signal to noise ratio is the highest at tool rotation angle φ = 90˚, corresponding to the maximum uncut chip thickness. Therefore, some inferences about the changes in cutting forces with process variables might be possible by studying the cutting force behavior at this particular rotation angle.

Figure 3 shows the variation of the tangential and radial forces with fiber cutting angle and rake angle for the tool rotation angle φ = 90˚. As shown in Table 1, the fiber cutting angles at this position for the four different laminates ψ = 0, 45, 90 and 135˚ are θ = 90, 135, 0/180 and 45˚, respectively. It can be seen that the tangential force is sensitive to changes in the rake angle, with the tangential force decreasing as the rake angle increases from -15 to 15˚. The radial force is not sensitive to the rake angle for fiber cutting angles of 45, 90 and 135˚, but it is highly sensitive for the fiber cutting angle 0/180˚. Furthermore, the radial force is much higher than the tangential force for the 0/180˚ and 45˚ fiber cutting angles and for all rake angles. These results are in good agreement with the cutting force behavior in orthogonal machining of UD-CFRPs as reported in references [2, 4].

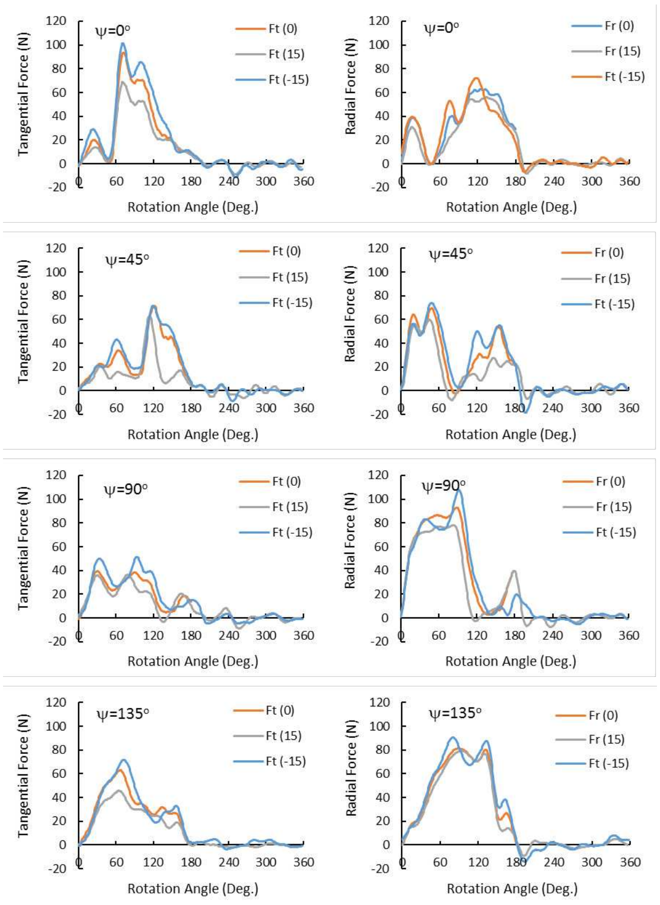

Figure 2. Variation of cutting forces with rotation angle for the different laminate orientations and rake angles used.

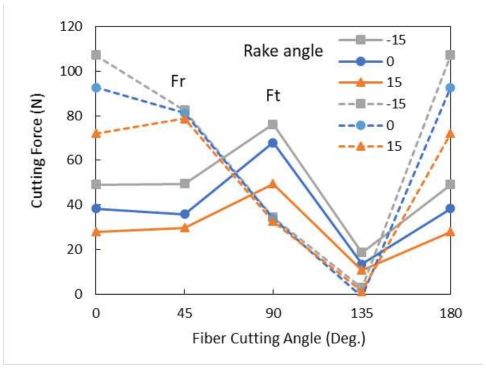

Figure 3. Effect of rake angle and fiber cutting angle of cutting forces at maximum uncut chip thickness *φ* = 90˚.

3.2. Friction behavior

Figure 4 shows a simplified cutting model according to [8]. In this model, the area ahead of the cutting edge is divided into two regions. Region 1 is the fiber cutting region where the fibers are sheared by the advancing cutting edge according to Merchant's minimum energy principle. The cutting forces in this region depend mainly on the fiber cutting angle and mechanical strength of the fibers, and they are independent of cutting edge wear. The fibers in Region 2 are not cut, but rather pressed by elastic deformation under the clearance face. The friction force in this region is proportional to the pressing force by the friction coefficient. The total cutting forces in the tangential and radial direction are the algebraic sum of the forces in the two regions,

$$\begin{aligned} F_t &= F_{t1} + F_{t2} = R_1 cos(\beta - \alpha) + \mu P \\ F_r &= F_{r1} + F_{r2} = R_1 sin(\beta - \alpha) + P \end{aligned} \qquad (4)$$

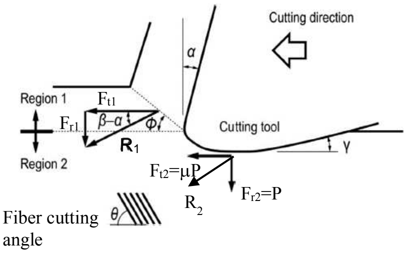

Figure 4. Simplified cutting model according to Maegawa et al. [8].

The pressing force in region 2 increases with the increase in edge radius due to tool wear. Thus, the change in the total cutting forces during milling can be represented only by the change in the forces in region 2, i.e. $\Delta F_{t2}=\mu\Delta P$ and $\Delta F_{r2}=\Delta P$. Subsequently, the coefficient of friction in region 2 can be estimated by the equation,

$$\mu = \frac{\Delta F_t}{\Delta F_r} = \frac{\Delta F_{t2}}{\Delta F_{r2}} \qquad (5)$$

Figure 5 shows the change in the cutting forces over time for the 90˚ laminate and 0˚ rake angle cutting tool. It can be seen that the most significant change in the cutting forces occurs in the radial component, possibly due to the increase in the pressing force caused by the cutting edge rounding. Figure 6 shows the ratio of the tangential force to the radial force for the 90˚ laminate and for different rake angles. The slopes of the regression lines in this figure represent the friction coefficients, μ for the different rake angles.

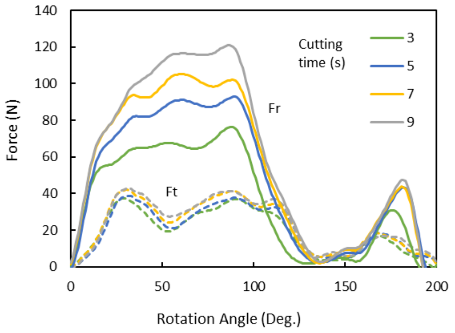

Figure 5. Change of cutting forces over time for laminate orientation ψ = 90˚ and rake angle α = 90˚.

The friction coefficient in milling UD-CFRP was estimated using the method outlined above for all combinations of laminate orientations and rake angles and the results are shown in Figure 7 as a function of the fiber cutting angle. It is noted that the same fiber cutting angle is obtained from different combinations of tool rotation angles and laminate orientations as shown in Table 1. However, for some rotation angles and laminate orientations (e.g. φ=135˚, ψ=0˚) the noise in the force signal was very high and estimation of the friction coefficient was not reliable. Therefore, each point in Fig.7 represents the average of friction coefficients obtained mainly from the combinations (φ=45˚, 90˚ and ψ=90˚, 135˚). Only one reliable data point could be obtained for the 0 and -15˚ rake angles at fiber cutting angle of 90˚.

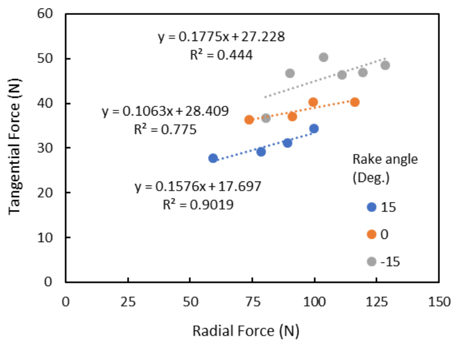

Figure 6. The ratio of tangential force over radial force for laminate orientation ψ = 90˚ and φ=90˚.

It is shown that the variation of μ with fiber cutting angle is extremely sensitive to the tool rake angle. For α = -15˚, μ varied slightly with fiber cutting angle from 0.12 to 0.25 and the lowest μ was at θ = 90˚. For the α = 0 and 15˚, μ varied significantly with fiber cutting angle where the highest μ = 0.84 occurred at θ = 90˚ for α = -15˚ and the lowest μ = 0.08 occurred at θ = 0/180˚ for α = 0˚. The high coefficient of friction in this case could be attributed to the severe bending and elastic spring back associated with the 90˚ laminate. To the contrary, the lack of bending and spring back associated with parallel fibers resulted in a low friction coefficient. Comparing the present findings with those reported in the literature [9-12], it can be concluded that the range of values of the friction coefficient and its relationship with fiber orientation shown in Fig. 7 are in good agreement, keeping in mind the differences in tool/FRP pairs used by the different sources. The reported friction coefficient increased from 0.3 to 0.9 with fiber inclination angle for HSS/GFRP [9], was 0.25 for CFRP/TiN coated carbide [10] and 0.32 for CFRP/uncoated carbide [12].

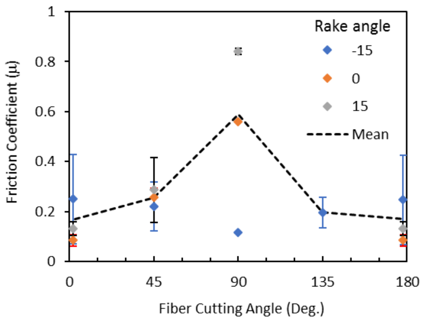

Figure 7. Variation of the friction coefficient with fiber cutting angle for different rake angles.

3.3. Force decomposition

Once the friction coefficient is determined, the resultant shearing force R_1 and pressing force P can be obtained by solving equations (4) as:

$$R_1 = \frac{F_t - \mu F_r}{cos(\beta-\alpha) - \mu\, sin(\beta-\alpha)} \qquad (6)$$

$$P = \frac{F_t sin(\beta-\alpha) - F_r cos(\beta-\alpha)}{\mu sin(\beta-\alpha) - cos(\beta-\alpha)} \qquad (7)$$

where the friction angle β is determined by:

$$\beta = tan^{-1}\mu \qquad (8)$$

Figure 8(a) shows the variation of the decomposed tangential shearing force F_{t1} and friction force F_{t2} with fiber cutting angle for the three rake angles used. Similarly, Figure 8(b) shows the variation of the decomposed radial shearing force F_{r1} and pressing force F_{r2}. Of the three rake angles, the tangential shearing force is the smallest for $\alpha = 15^\circ$, indicating very efficient cutting of the fibers with this angle. This is due to favorable conditions for continuous chip formation and the reduced deformation to the fibers [1, 2]. The influence of the rake angle is most significant at 90° fiber cutting angle. At this angle, the friction force for the positive rake angle tool is the highest. The tangential shearing force and friction force are comparable in magnitude for the 0/180° fiber cutting angle. On the other hand, the pressing force is much larger than the radial shearing force for 0/180° and 45° fiber cutting angles. The smallest friction forces and smallest pressing forces occur for fiber cutting angles of 90 and 135°. At these particular fiber orientations, the cut fibers move away from the tool clearance face as they bounce back, causing less pressure on the tool face.

3.4. Relationship to machining damage

Machining damage in milling UD-CFRP occurred mainly in the form of overhanging uncut fibers (fuzzing) and cracking of the laminate as shown in Fig. 9. Table 2 shows the range of fiber cutting angles at which fuzzing was observed for the different laminate orientations and rake angles. The corresponding tool rotation angles are also shown between parentheses. Fuzzing was more frequent than cracking and occurred mostly for 0°, 45° and 135° laminate orientations. Fuzzing and cracking were also associated more with the negative rake angle tool due to the higher cutting forces. For the 0° laminate fuzzing was observed at the tip of the cutting circle ahead of the cutting tool. Cracking occurred mostly for the 45° and 90° laminates and appeared always on the down-milling side. For the 45° laminate fuzzing was observed on the up-milling and down-milling sides, while for the 135° laminate it appeared only on the up-milling side. Table 2 shows that fuzzing occurred mostly in the fiber cutting angle range from 120° to 20° for the negative and zero rake angle tools. This observation is consistent with the findings of Wang et al. [5] and Voss et al. [6]. For the positive rake angle tool, fuzzing occurred in a much narrower range of fiber cutting angles on the up-milling side of the slot.

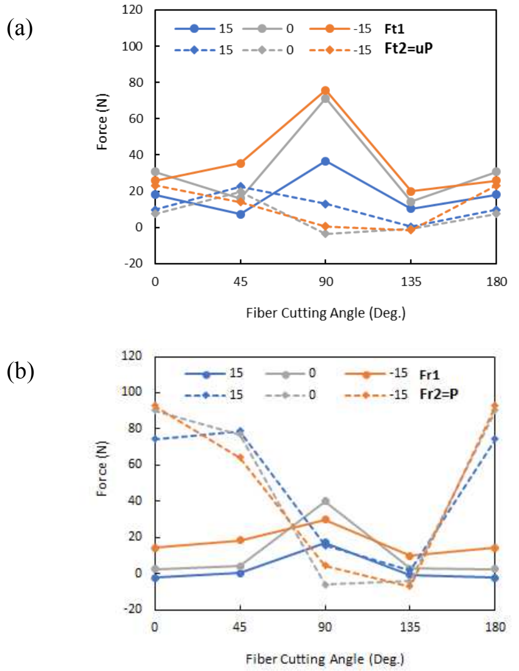

Figure 8. Variation of the tangential (a) and radial (b) cutting force components in the shearing and pressing regions, respectively ($\varphi = 90^o$).

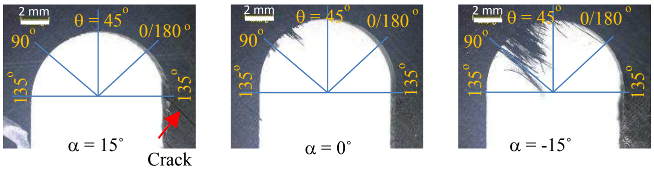

Figure 9. Fuzzing and cracking damage when milling laminate orientation ψ = 135°.

Table 2. Cutting fiber angle ranges at which fuzzing was observed. Corresponding tool rotation angles are shown between parentheses

	ψ (Deg)			
α (Deg)	0	45	90	135
-15	120-30° (60-150°)	115-45° (110-180°)	-	105-25° (30-110°)
0	115-20° (65-160°)	-	-	105-65° (30-70°)
15	-	45-5° (0-40°)	75-50° (15-40°)	-

The relationship between machining damage and cutting forces is explained by studying the resultant cutting force magnitudes and orientations as shown in Figures 10 and 11. The resultant force in region 1, R_1, makes an angle $(\beta-\alpha)$ with the cutting speed vector and an angle χ with the fibers. The total resultant force, R makes an angle λ with the cutting speed vector. The resultant force in region 2, R_2, assumes an orientation which is uniquely determined by the orientations of R_1 and R. The magnitudes and orientations of the three resultant forces change continuously with the rotation angle as shown in Figure 11 for the 135° laminate.

As shown in Table 2, fuzzing appears for the 135˚ laminate in the tool rotation angle range of 30-110˚ for the negative rake tool and 30-70˚ for the zero rake tool. These ranges are characterized by increasingly high shearing forces and high inclination angles χ as shown in Figure 11. Similar conditions were also found for the other laminate orientations. According to [4] and [6], the occurrence of overhanging uncut fibers is caused by the fiber behaving as a cantilever beam which evades cutting by bending out of plane ahead of the cutting edge. This behavior is obviously promoted by high cutting forces which act transverse to the fiber (i.e. χ is in the neighborhood of 90˚). On the other hand, shallow angles promote fiber cutting due to the combined effect of stretching and shearing, and thus fiber bending is less likely. For instance, the inclination angle of R_1 for the positive rake angle tool is high, but its magnitude is very low, and therefore fuzzing does not occur due to insufficient bending force. Also, for tool rotation angles greater than 110˚, the inclination angle of R_1 drops significantly and fuzzing disappears due to the combined effect of stretching and shearing. Therefore, it can be concluded from this observation that a necessary condition for overhanging fibers to occur is that the magnitude of the shearing force R_1 must by sufficiently high and its inclination angle χ is closer to the perpendicular.

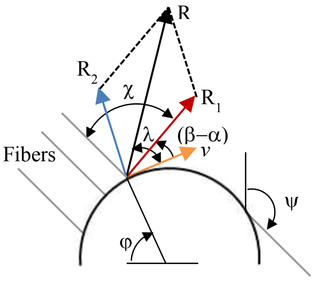

Figure 10. Resultant cutting forces and their orientation.

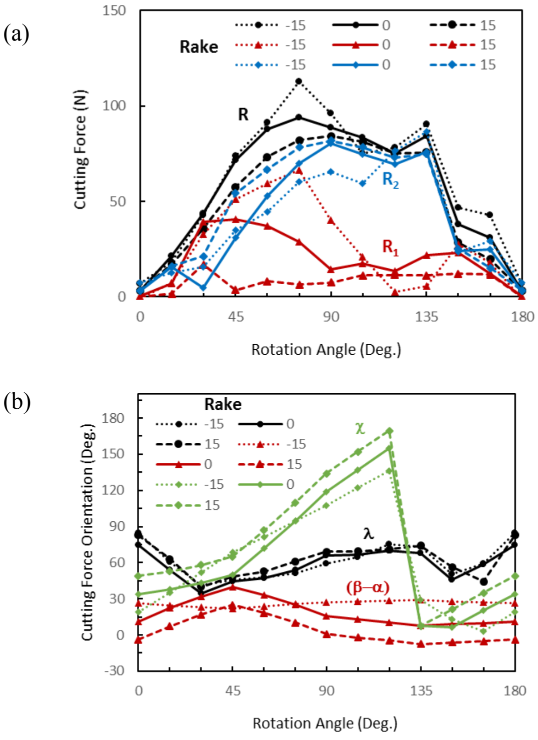

Figure 11. Evolution of the resultant cutting forces (a) and their orientation (b) during one revolution for ψ = 135˚.

Conclusions

Cutting forces in slot milling of UD-CFRP were analyzed using a two-regions cutting model and correlations were made between machining damage and the magnitude and direction of the shearing force. The main conclusions of this work are:

- The estimated coefficient of friction on the clearance face depends on the fiber cutting angle, with the average peaking at $\theta = 90˚$.
- From cutting force, surface integrity and tool wear perspectives, tools with $\alpha \geq 0˚$ are ideal.
- Machining damage most likely occurs in the form of overhanging fibers when the resultant shearing force is sufficiently and high and its orientation is transverse to the fibers.

Acknowledgment

Authors would like to thank OSG Corporation for providing tooling for this research project.

References

[1] Kaneeda T. CFRP cutting mechanism. In Proceeding of the 16th North American Manufacturing Research Conference 1991. p. 216-221.

[2] Wang DH, Ramulu M, Arola D. Orthogonal cutting mechanisms of graphite/epoxy composite. Part I: Uni-directional laminate. International Journal of Machine Tools and Manufacture 1995;35 (12):1623-1638.

[3] Wang XM, Zhang LC. An experimental investigation into the orthogonal cutting of unidirectional fibre reinforced plastics. International Journal of Machine Tools & Manufacture 2003;43 (10):1015-1022.

[4] Hintze W, Hartmann D, Schütte C. Occurrence and propagation of delamination during the machining of carbon fibre reinforced plastics (CFRPs) – An experimental study. Composites Science and Technology 2011;71 (15):1719-1726.

[5] Wang, F-J, Yin, J-W, Ma, J-W, Jia, Z-Y, Yang, F, Niu, B. Effects of cutting edge radius and fiber cutting angle on the cutting-induced surface damage in machining of unidirectional CFRP composite laminates. Int J Adv Manuf Technol 2017; 91:3107-3120.

[6] Voss R, Seeholzer L, Kuster F, Wegener K. Influence of fibre orientation, tool geometry and process parameters on surface quality in milling of CFRP. CIRP Journal of Manufacturing Science and Technology 2017; 18:75-91

[7] Zhang LC, Zhang HJ, Wang XM. A force prediction model for cutting unidirectional fibre-reinforced plastics. Machining Science and Technology 2001;5 (3):293-305.

[8] Maegawa S, Morikawa Y, Hayakawa S, Itoigawa F, Nakamura T. Mechanism for changes in cutting forces for down-milling of unidirectional carbon fiber reinforced polymer laminates: Modeling and experimentation. International Journal of Machine Tools and Manufacture 2016;100:7-13.

[9] Nayak D, Bhatnagar N, Mahajan P. Machining studies of UD-FRP composites Part 2: Finite element analysis. Machining Science and Technology 2005;9 (4):503-528.

[10] Klinkova O, Rech J, Drapier S, Bergheau J-M. Characterization of friction properties at the workmaterial/cutting tool interface during the machining of randomly structured carbon fibers reinforced polymer with carbide tools under dry conditions. Tribology International 2011;44 (12):2050-2058.

[11] Voss R, Seeholzer L, Kuster F, Wegener K. Cutting process tribometer experiments for evaluation of friction coefficient close to a CFRP machining operation. Procedia CIRP 2017;66:204-209.

[12] Xu, J., Li, C., El Mansori, M., Liu, G., Chen, M. Study on the Frictional Heat at Tool-Work Interface when Drilling CFRP Composites. Procedia Manufacturing 2018; 26:415–423.